# Poincaré's Section Analysis of Photoplethysmography Signals for Cuff-Less Non-Invasive Blood Pressure Measurement

**Fatemeh Shoeibi**
Sahand University of Technology
**Esmaeil Najafiaghdam** (✉ najafiaghdam@sut.ac.ir)
Sahand University of Technology https://orcid.org/0000-0002-7803-998X
**Afshin Ebrahimi**
Sahand University of Technology

**Research Article**

**Keywords:** Hypertension, Poincaré's section, Photoplethysmography, Non-invasive, Cuff-less, Blood pressure monitoring.

**Posted Date:** February 15th, 2021

**DOI:** https://doi.org/10.21203/rs.3.rs-171469/v1

# Poincaré's section analysis of Photoplethysmography signals for cuff-less non-invasive blood pressure measurement

**Fatemeh Shoeibi[a], Esmaeil Najafiaghdam[b*], Afshin Ebrahimi[c]**

[a] Department of Electrical Engineering, Sahand University of Technology, Tabriz, Iran

[b*] Department of Electrical Engineering, Sahand University of Technology, Tabriz, Iran

[c] Department of Electrical Engineering, Sahand University of Technology, Tabriz, Iran

## Abstract

**Background and Objective:** Hypertension is a serious problem that has become dramatically more common in recent decades. Hypertension can be managed in its early stages by regular monitoring of blood pressure. Blood pressure, as a vital signal, has an essential role in the prediction of many cardiovascular diseases. Therefore, non-invasive, cuff-less, continuous monitoring of blood pressure has special importance in personal health care. Recently, due to the capabilities of PPG sensors in embedding and compacting as a wearable device, application of the PPG signal and its characteristics as a useful facilities for BP measurement have been highlighted. **Methods:** This study attempts to provide a new indicator of PPG waveforms to help the rapid developments in this research area. The proof of the feasibility of using Poincaré's section for extracting the profitable features of the PPG signal for BP estimation is one of the key achievements of this paper. **Results:** The performance of the method was evaluated on 101 subject's clinical data from the MIMIC □□ database. The proposed method obtains a mean absolute error of 2.1 mmHg for systolic pressure and 1.4 mmHg for diastolic pressure prediction. Also, the results meet the AAMI and BHS standards, which demonstrate the feasibility of Poincaré's section-based indices in BP estimation. **Conclusions:** The results confirm the proficiency of this method in the blood pressure estimation and a straightforward way to reduce the computational and hardware complexity, which in turn helps to achieve a real-time wearable BP monitoring system.

**Keywords:** Hypertension, Poincaré's section, Photoplethysmography, Non-invasive, Cuff-less, Blood pressure monitoring.

**Abbreviations:** Diastolic Blood Pressure(DBP); Blood Pressure(BP); Systolic Blood Pressure(SBP); Mean Absolute Error(MAE); Standard Deviation(STD); Association for the Advancement of Medical Instrumentation(AAMI); BHS, British Hypertension Society(BHS); Photoplethysmography(PPG); Pulse

* Corresponding author at: Department of Electrical Engineering, Sahand University of Technology, Tabriz, Iran.

E-mail address: najafiaghdam@sut.ac.ir

Transit Time(PTT); Arterial Blood Pressure(ABP); Pulse Wave Velocity(PWV); Impedance Plethysmography(IPG); Photoplethysmogram Intensity Ratio (PIR); Stiffness Index (SI); Body Mass Index (BMI) .

## 1. Introduction

Hypertension, which is often the result of recent changes in lifestyle, is a prominent cause of cardiovascular diseases. Therefore, the demand for non-invasive, continuous systems that can monitor the BP changes without interrupting people's daily activities has grown considerably. Considering the importance of preventative strategies, providing non-invasive detective method has become an urgent requirement for personal health monitoring purposes. The most common way is the use of cuff-based systems that are discontinuous, inconvenient, and obtrusive for long-time measurements. Recently, the research in developing BP monitoring systems without cuff has become the focus of researchers[1]. Lastly, in a comprehensive investigation, the reported systems and methodologies on non-invasive cuff-less blood pressure measurement were reviewed. Moreover, the review focused on the challenges that have to be still overcome to optimize the currently proposed systems to emerge as an accurate and reliable clinically cuff-less monitoring system. [2].The use of biological signals such as PPG and ECG for BP monitoring has rapidly grown over the past few years[3, 4]. Among these, PTT and PWV based methods have become more prominent [5–7].

PWV and PTT are two cardiovascular parameters which have a high correlation with BP [8]. PTT refers to the time interval that the pressure pulse takes to propagate from the heart to the arterial tree. In practice, PTT is usually introduced as the time distance between two specific points on two physiological signals, such as two PPG signals[9, 10], ECG and PPG[5], or IPG and PPG signals[11]. In general, PTT is computed as the time distance between a maximum amplitude or minimum valley on the PPG signal and the R peak of an ECG signal [12]. A wide variety of models have been presented to make clear the relationship between blood pressure and PTT[8]. A thorough literature review on current and proposed methods for BP monitoring via PTT and their limitations is presented in[13]. In this article, researchers have tried to explain foundational models for the theory of the PTT-BP relationship. In another comprehensive study[14], researcher provides a review on the state of the art models which have been explored in the literature to explain the relevance of BP with PTT.

Physiological and biomedical subject-dependent parameters which influence the cardiac system and thus, in turn, affect BP can be combined with PTT-based features to improve the BP estimation accuracy. The results of the survey on the impact of adding hemodynamic covariates such as heart rate (HR) and arterial stiffness index (SI) on the PTT-base feature for BP estimation elucidate that, by incorporating SI, which is defined as the time interval between maximum peak on the PPG signal and maximum peak on the dicrotic notch, along with HR and other hemodynamic covariates the accuracy of estimation improved significantly[15]. In a recent survey on BP measurement, the application of the PTT and photoplethysmogram intensity ratio (PIR), along with the Womersley

number, which reflects the effect of blood flow specifications as a significant and impressive feature on BP accuracy, was reported by researchers in[16]. In some researches, using only the ECG signal for blood pressure estimation has been investigated. For example, in[17], after extracting the R peaks in the ECG signal, the Fourier transform was applied to the signal between two R peaks to extract whole based frequency domain features.

The PPG signal has many informative features about the cardiovascular system and personal health status[18, 19]. In a gainful trial, the intrinsic physiological characteristics of the PPG signal were explored. The result confirms that the most commonly used morphological and time-domain features of the PPG signal for BP estimation have a high correlation with SBP and pulse pressure. The outcomes of this survey clarify the fact that the PPG signal features have significant potential to be exploited in BP estimation applications[20]. Moreover, regarding the research on cuff-less BP estimation, several efforts were devoted to develop a blood pressure system by using only PPG signals[9]. This signal indicates the blood volume changes caused by cardiovascular system activity, which is closely related to blood pressure variation and can be affected by factors that affect blood pressure. The PPG signal can be measured from different points such as wrist, fingertip and ears. As an example, in [9], the synchronous recorded PPG signals from wrist and fingertip were employed for BP measurement purpose. The authors performed a feature analysis employing the genetic algorithm to select the most important features for BP estimation.

Researchers have become intensely interested in the PPG signal due to the simplicity of the PPG sensor and its ability to be configured as a wearable system with high comfort for users and because of its advantages as a non-invasive, low-cost diagnostic tool[9]. These sensors have the potential to be a single point measurement. The PPG sensor does not have any requirement to gel, and its ease of usage increases the adoption of this sensor for wearable BP measurement purposes. The application of a single PPG sensor could be a reasonable suggestion to get rid of the difficulty of applying several sensors on the subject's body. All of the benefits mentioned above make this sensor a perfect and prevalent tool in designing and making wearable health monitoring systems.

Due to these advantages, the PPG signal has attracted huge attention in cuff-less BP measurement[21]. A comprehensive overview of issues related to the BP monitoring systems that attempt to measure blood pressure using PPG signal in a cuff-less and non-invasive technique has been provided in[22]. The most critical challenges such as PPG signal receiver design consideration, motion artifact problem, selecting the best machine learning algorithms to optimize the accuracy of BP estimator was demonstrated. Moreover, a comprehensive review of machine learning techniques for BP estimation from the PPG signal has been conducted in[23]. In a valuable work, researchers have explored the capability of a PPG signal to be used as a surrogate of the Arterial Blood Pressure (ABP). They perform similarity analysis in both frequency and time domains between PPG and ABP waveforms. Highly correlation coefficient in the time-domain between two mentioned signals confirm the potential of the PPG pulses as a possible substitution for invasive ABP[24]. The application of the PPG signal as a smartphone-based method for heart rate and BP estimation was investigated in[25]. In some surveys based on the PTT method,

researchers attempt to improve the accuracy of BP estimation using photoplethysmogram intensity ratio (PIR) index. PIR index is defined as the peak intensity to the valley intensity ratio in the PPG signal and reflects the vessel diameter variation during each cardiac cycle from systole to diastole[6].

A wide variety of researches have been conducted using time and amplitude domain or frequency domain features of the PPG signal for BP estimation, which is known as parameter-based features[26, 27]. In another survey, a different set of feature extraction algorithms, which is called a whole-based method, was employed to extract indices regardless of the PPG signal shape. According to the whole-based method reported in[28], raw values between two successive systolic peak in the PPG signal is selected as a feature set and is conducted to the machine learning algorithm. Unfortunately, these methods require some computational effort for accurate detection of local points, especially regarding dicrotic notch in old subjects with damped PPG signal[29, 30]. The first and second derivatives of PPG signal (APG) have the potential to provide informative and highly correlative features with BP. The impressive role of extracting features from the APG signal on the accuracy of BP measurement was explored in[31]. Aiming to prevent high blood pressure, The application of time-domain features from the first and second derivative of the PPG signal for calibration-free BP estimation has also been investigated in[32]. The authors designed an optimized inductive algorithm to estimate SBP and DBP which utilizes both sequential and parallel ensemble machine learning algorithms to increase estimation accuracy.

Despite the approved performance of the mentioned methods in BP measurement, these methods are involved with the complexity of detecting points on the waveform, especially regarding the second derivative, which hardly can be identified the sufficient number of expected peaks, thus revealing the fact that those features are unusable. Additionally, variable physiological parameters and age can cause changes in the morphology of PPG signals, causing the complexity of determining proper features for BP estimation[33].

In the present paper, we have tried to develop a novel algorithm for BP estimation using Poincaré's section analysis of PPG signals. Given the challenges mentioned above, the proposed method tried to overcome the computational complexity and solve the problems mentioned in other methods. Recruiting Poincaré's section analysis for feature extraction has the advantage of releasing the requisites for precise detection of local points in the PPG signal. The paper is organized as follows: a detailed description of the proposed method, including signal preprocessing, feature extraction, and nonlinear machine learning is explained in Section 2. The results of a novel method using two learning algorithms and the advantages of this work are provided in Section 3. Section 4 provides a discussion about the proposed method. In the end, the concluding section summarizes the outcomes of the purposed method.

## 2. Methods

In this study, we employed only the PPG signal for the BP measurement purpose in a non-invasive, cuff-less manner. The novelty of this attempt is the introduction of a new algorithm to estimate BP to achieve more accurate estimations. For this purpose, Poincaré's section analysis of the PPG signal is applied to extract the most important features of the PPG signal for BP estimation. The effectiveness of Poincaré-based features of the PPG signal was confirmed in emotion recognition[34]. The proven potential of Poincaré's sections as a powerful tool for dynamic behavior analysis of a system conveys the fact that this opportunity could be a sensible incentive for its application in the BP estimation. Since human blood pressure has dynamic behavior, herein, the idea of using Poincaré's section for investigating the variation of such a dynamic system was proposed. The accomplishment process of the proposed method is summarized in the block diagram in **Fig 1**.

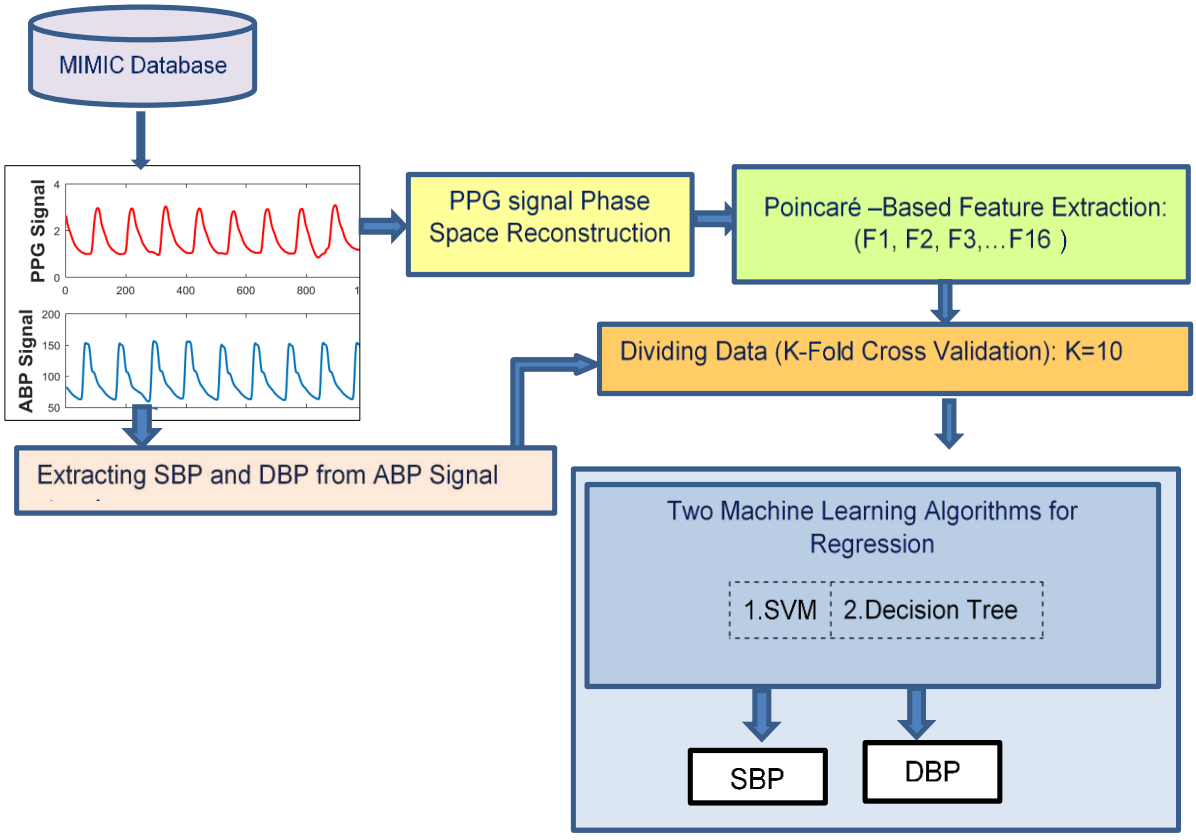


**Fig 1**. Block diagram of the proposed method

As shown in **Fig 1,** the following steps are used to extract features:

- In the preprocessing step, the noise of the PPG signal was removed.

- The PPG signal for every subject was segmented. The length of each segment was 8s. Since the sampling frequency of the signal according to MIMIC database reports was 125 Hz, the size of each segment was 1000 samples. Each segment contains at least 8 PPG pulse cycles. Simultaneously, in each window of the ABP signal, the values of systolic and diastolic pressure were extracted as a reference. This step was performed through finding peaks and valleys in the ABP waveform.
- For every window, the 2D phase space of the PPG signal was reconstructed by selecting PPG signal as X-axis and time-delayed PPG signal as Y-axis. The size of the delay in this work is 15 samples. Then Poincaré's section was formed.
- Profitable and informative indices of phase space plane were extracted from Poincaré's sections.
- Extracted features were provided to the machine learning blocks to estimate systolic and diastolic BP separately.

In the end, the accuracy of the predicted values for SBP and DBP was evaluated according to the ANSI/AAMI SP-10 standard for non-invasive BP measurement techniques.

## 2.1. Databases

In this paper, the data of Multi Parameter Intelligent Monitoring in Intensive Care (MIMIC)II (version 3, 2015)[12] online waveform was used, which was provided by the PhysioNet organization[35]. The data contains clinical records for subjects, such as PPG, ECG and ABP signals that in the current work, the PPG and APB signals of 101 subjects were used for evaluating the proposed method. These signals were sampled at the frequency of 125Hz which have the minimum accuracy of 8-bit. The reference systolic and diastolic blood pressure values were extracted from ABP signal. The PPG signal was utilized to exploit proper features to apply for training and testing the machine learning models. Statistical information related to these 101 subjects is illustrated in **Fig 2**. The plot exhibits that the SBP and DBP data were distributed in a wide range from very low to very high values, which makes it possible to assess the power of the proposed method for BP estimation, effectively. This database did not provide the subject's physical information such as age and BMI.

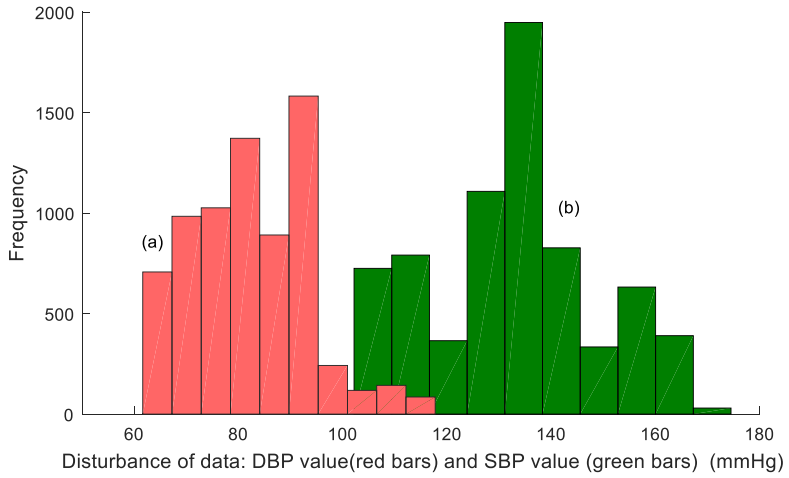


**Fig 2**. Histogram of database (a) DBP (b) SBP

## 2.2. Preprocessing

In this stage, the signal preprocessing was carried out by noise removing and segmentation. As mentioned earlier, both PPG and ABP signals were divided into intervals of 8s. High-frequency noises due to muscular activities were eliminated using a low-pass filter with a cutoff frequency of 15Hz and low-frequency components were removed using a high-pass filter with a cutoff frequency of 0.5 Hz. A Third-order Butterworth band-pass filter (0.5 Hz-15 Hz) was employed for this step. Furthermore, baseline modulation was removed from the PPG data. This baseline wander can be a result of losing body and sensor contact due to the subject's unwanted movement during measurement or because of abnormal breathing [36].

Then preprocessing is continued by eliminating unreliable segments that deteriorated due to different distortions and artifacts. As an example, segments that have abnormal PPG waveform and acceptable waveform have been depicted in Fig 3(a) and Fig 3(b), respectively. The autocorrelation between successive pulses in each segment, as similarity criteria, was calculated to discard segments with high alteration or severe discontinuities, which were not improved by smoothing and using an averaging filter. In total, the numbers of acceptable signal segments were 7150. In the next stage, the amplitude of the cleaned PPG signal in each segment was normalized. By normalizing signals according to Eq (1), PPG signal (S) would be in the range of [0, 1]. After preprocessing, the clean data is used as input to feature selection block.

$$\text{Normalized PPG} = \frac{S - \min(S)}{\max\ (S) - \min(S)} \tag{1}$$

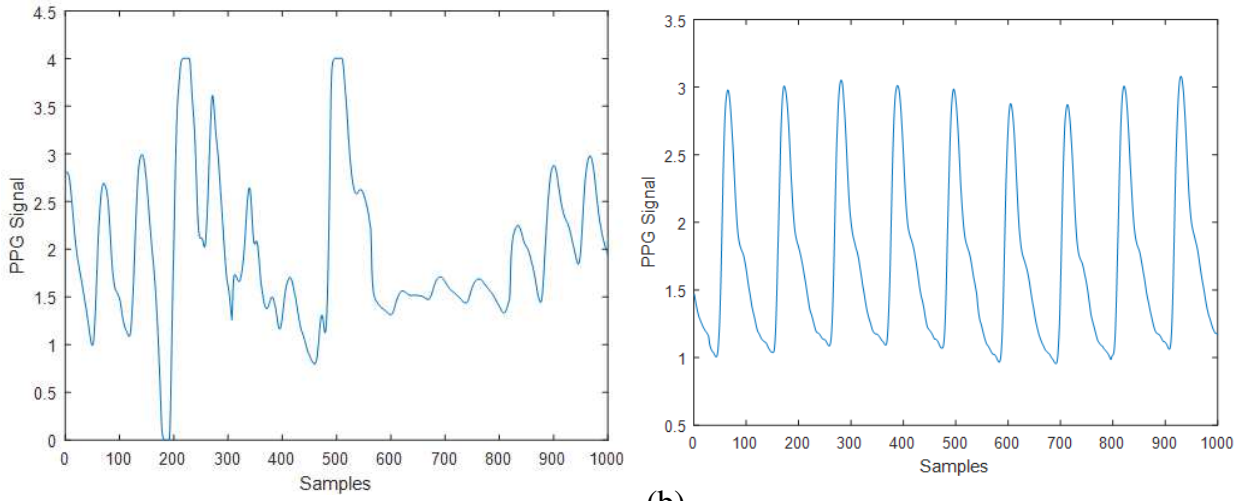


(a) (b)

**Fig 3.** An abnormal PPG waveform from MIMIC database (a) normal PPG signal (b)

## 2.3. Phase space and Poincaré's section

### 2.3.1. Phase space creation strategy

The reconstruction of phase space is necessary for creating Poincaré's section. Given $x=\{x_1,x_2,....,x_n\}$ as one-dimensional PPG signal, phase space of the signal is defined as Eq(2) [37]:

$$\dot{x}=\begin{bmatrix} x_{1+(m-1)\tau_d} & \cdots & x_{1+\tau_d} & x_1 \\ x_{2+(m-1)\tau_d} & \cdots & x_{2+\tau_d} & x_2 \\ \cdot & & \cdot & \cdot \\ \cdot & & \cdot & \cdot \\ x_n & & x_{n-(m-1)\tau_d} & x_{n+(m-1)\tau_d} \end{bmatrix} \quad (2)$$

Where, $\dot{x}$ represents the m-dimensional trajectory matrix, $\tau_d$ is the time lag, and m is the embedding dimension. The matrix $\dot{x}$ is mapping the one-dimensional signal to an m-dimensional system to reconstruct the phase space attractor. The delay $\tau_d$ can be estimated from the correlations among PPG samples.

### 2.3.2. Poincaré's section

Consider the reconstructed m-dimensional trajectory $\dot{x}$ from the scalar PPG waveform $x$ which is defined in subsection 2.3.1, the intersections of a trajectory with a specific (m-1)-dimensional

subspace (hyper plane) in the phase space, give the sense of a Poincaré's section[38]. In other word, marking the points where the signal trajectory crosses these sections creates a mapping called Poincaré's section.

In the current paper, the phase plane of the PPG waveform was reconstructed by time delaying of signal S. The appropriate lag value was applied to create a time-delayed signal, S (t + τ). The selection of very large or very small values for lag affects the quality of the phase map. The detailed considerations related to lag size selection could be investigated in[39], in which mutual information was introduced as a criterion for choosing the lag value. The procedure for forming the phase plane to create Poincaré's section is as follows[34]:

- Two-dimensional phase space (m=2), was reconstructed by selecting the PPG signal as X-axis and the time-delayed PPG signal S (t + τ) as Y-axis. Through trial and error, the size of delay in this work was set to 15 samples.
- After the reconstruction of phase space, selection of the Poincaré hyper plane is the next step. Poincaré section in two-dimensional phase space was created by crossing lines in the angle θ with a signal trajectory. In this study, θ varies with a step size of 30° in the range of [0°, 360°]. The points where the signal trajectory crosses the lines are defined as the Poincaré's sections. The details about how the crossing points are detected can be read in[34]. **Fig 4** illustrates Poincaré representation of one segment of the PPG signal in a phase plane.

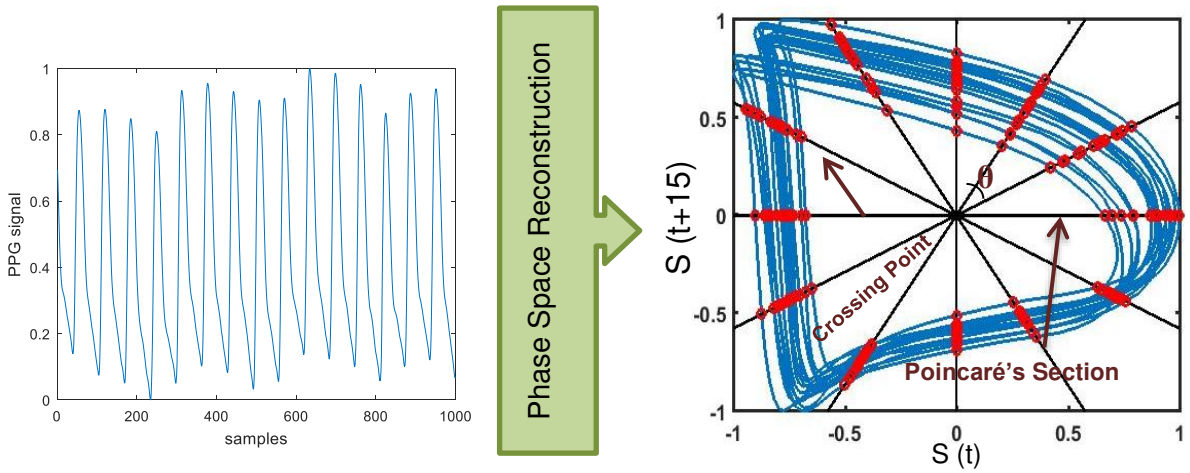


**Fig 4.** The reconstructed phase space and trajectory of one cycle of PPG signal .The black lines refer to Poincaré's sections and the red circles show the crossing points of Poincaré's sections with data trajectory

## 2.4. Feature Extraction

One thing worth noting is that using this novel method, there is no need to find the dicrotic notch. Therefore, even PPG signals that this point is not detectable can be used for feature extraction. In the next step, the proper indices were extracted from the Poincaré's sections, as shown in Table1.

**Table 1**
The extracted features from PPG signals in the reconstructed phase space

| Features | Description |
|---|---|
| **F1** | The number of points in the signal trajectory that cross the lines (red circles as illustrated in **Fig 4**) |
| **F2,F3** | The mean and standard deviations of X-coordinates of crossing points |
| **F4, F5** | The mean and standard deviations of Y-coordinates of crossing points |
| **F6** | The standard deviations of data in X-coordinates (STD of S $(t + \tau)$) |
| **F7** | The standard deviation of data in Y-coordinates (STD of S) |
| **F8,F9** | The skewness and kurtosis of X-coordinates of crossing points |
| **F10, F11** | The skewness and kurtosis of Y-coordinates of crossing points |
| **F12, F13** | The skewness and kurtosis of data in Y-coordinates |
| **F14, F15** | The skewness and kurtosis of data in X-coordinates |
| **F16** | The area under blue curves for each PPG segment |

In total, 16 features were extracted from Poincaré's sections. These features were applied to the machine learning regression algorithms to estimate the SBP and DBP.

The extracted features from the phase-plane analysis of the PPG signals were applied to the non-linear regression model to estimate BP. 10% of the input features were considered as a test set, and the rest of data allotted to the model learning. In this study, two machine learning algorithms (regression tree and SVM) were employed to estimate BP. The performance of two methods (SVM, Decision tree) was evaluated by 10-fold cross-validation.

#### 2.4.1. SVM Based Regression (SVR)

Support Vector Machine (SVM) is a powerful tool for solving the problems of non-linear classification and function estimation which uses kernel-based statistical learning methodology for this purpose. The main idea of SVM is based on mapping input feature data onto a high dimensional feature space using kernel functions and then linearly solving non-linear problems. This kernel function can be RBF, polynomial and sigmoid kernel function. Because of non-linear nature of SVM, it has great potential for employing complicated characteristics of human physiological signals to estimate blood pressure. So, in this study, the feature space F= (F1, F2….F16) was transformed into a new feature space using RBF kernel function to form a non-linear mapping model between the physiological data and BP. After training the SVM regression model using the training data set with the aim of getting the optimal model parameters to minimize the error function between the estimated and reference BP, the trained SVM model can be employed to predict BP using test data.

#### 2.4.2. Decision Tree for Regression

This regression model uses a multilevel structure that resembles the branch of a tree to reach a target value based on a training data set. The regression tree begins with one node (root) and in this node, the most important factor in determining the target value (BP in this case) is selected.

Then it branches into two or more descendant nodes according to a predetermined splitting criterion. Following the same procedure, to get the highest resolution each decision node is branched at the best point. In this model, the leaves of the tree represent target values, and each node refers to a feature or trait and the branch from each node shows the outcome of that node [40].

## 3. Results

To prove the efficiency of the phase characteristic of the PPG signal in BP estimation, the sum of 16 features using Poincaré's sections was extracted. Susceptibility of these features for BP estimation was investigated using two machine learning techniques. For each regression model 10-fold cross-validation was conducted. **Fig 5** indicates the histograms of estimation error using SVM-based regression. The histograms of error between the predicted value and real value using decision tree regression are exhibited in **Fig 6**. According to the histograms, error values for SBP and DBP are normally distributed around zero. Besides this, as shown in **Fig 6**, there is a high density of error around zero for decision tree regression model that shows the estimated BP value agrees closely with target values, which proves the ability of decision tree regression model for BP estimation using the phase-space feature set.

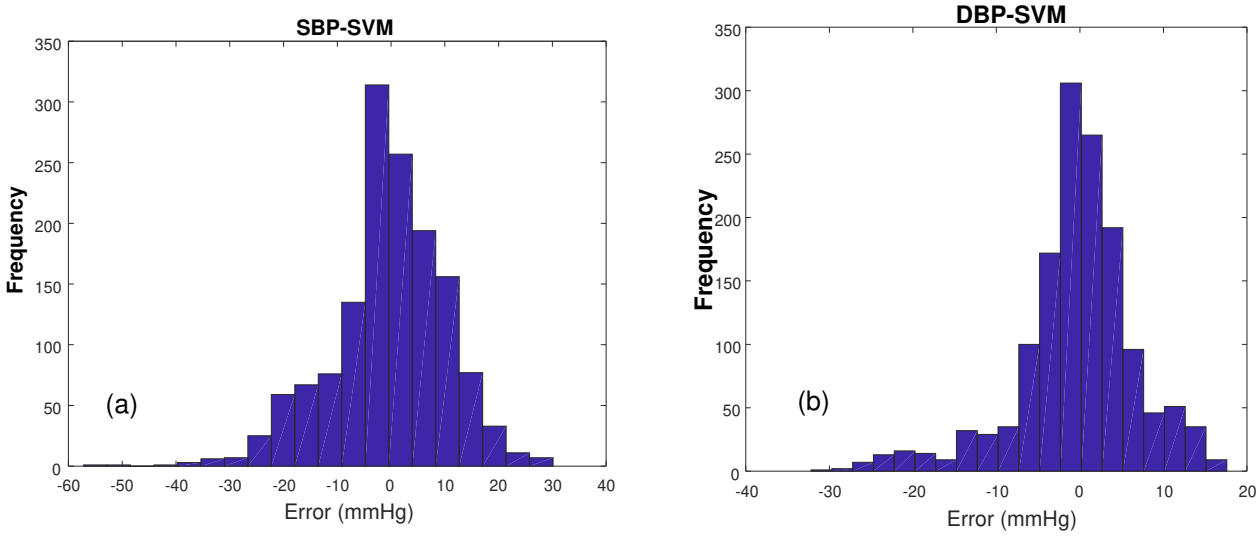


**Fig 5**. BP error histogram from the SVM regression, a) SBP b) DBP

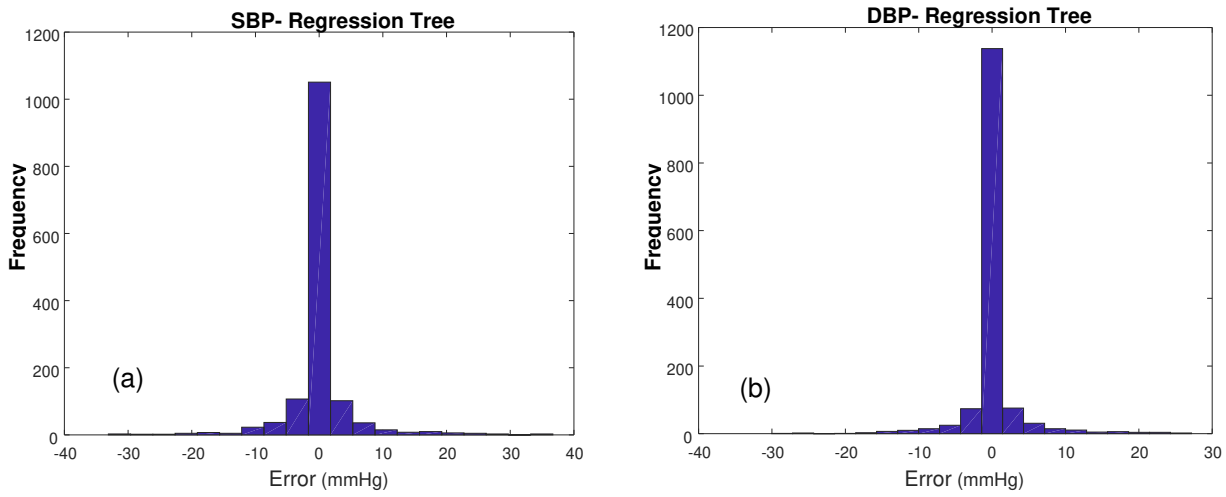


**Fig 6**. BP error histogram from the decision tree a) SBP b) DBP

## 3.1. Machine Learning Algorithm selection

The performance results of our method for BP estimation using two machine learning algorithms, is presented in Table 2. The correlation coefficient (r), MAE and STD are used as criteria for selecting the best learning model. Based on the result in Table 2, it is clear that the decision tree has a higher correlation coefficient compared to SVM method, which indicates the capability of this model in BP estimation. Also, **Fig 7** shows a comparative representation of three performance evaluation metrics for two regression method. **Fig 8** depicts the Bland Altman illustrations for SBP and DBP values. The Bland-Altman plot provides a comparative representation of predicted BP versus the reference BP and indicates the agreement between reference BP values and estimated BP values. In other words, Bland-Altman illustrates the differences between real BP and estimated BP values on the Y-axis against the average of the real BP and estimated BP values on the X-axis. As presented in **Fig 8**, the limits of agreement (mean ±1.96×STD) for SBP are (0.1 ± 9.98) mmHg and for DBP are (0.13 ± 7.4) mmHg.

**Table 2**
Performance evaluation between two machine learning algorithms

| | **Systolic blood pressure** | | | | **Diastolic blood pressure** | | | |
|---|---|---|---|---|---|---|---|---|
| **Regression Method** | ME (mmHg) | MAE (mmHg) | STD (mmHg) | r | ME (mmHg) | MAE (mmHg) | STD (mmHg) | r |
| **Support Vector Machine** | 0.35 | 7.9 | 10.64 | 0.74 | -0.39 | 5.04 | 7.15 | 0.77 |
| **Decision Tree** | 0.108 | 2.1 | 5.09 | 0.95 | 0.13 | 1.4 | 3.79 | 0.94 |

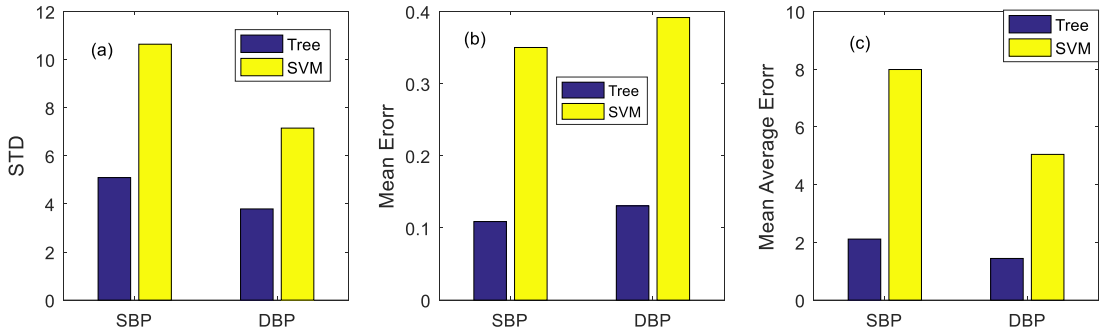


**Fig 7**. Comparison of three performance metrics for SVM and Decision Tree a) STD b) ME c) MAE

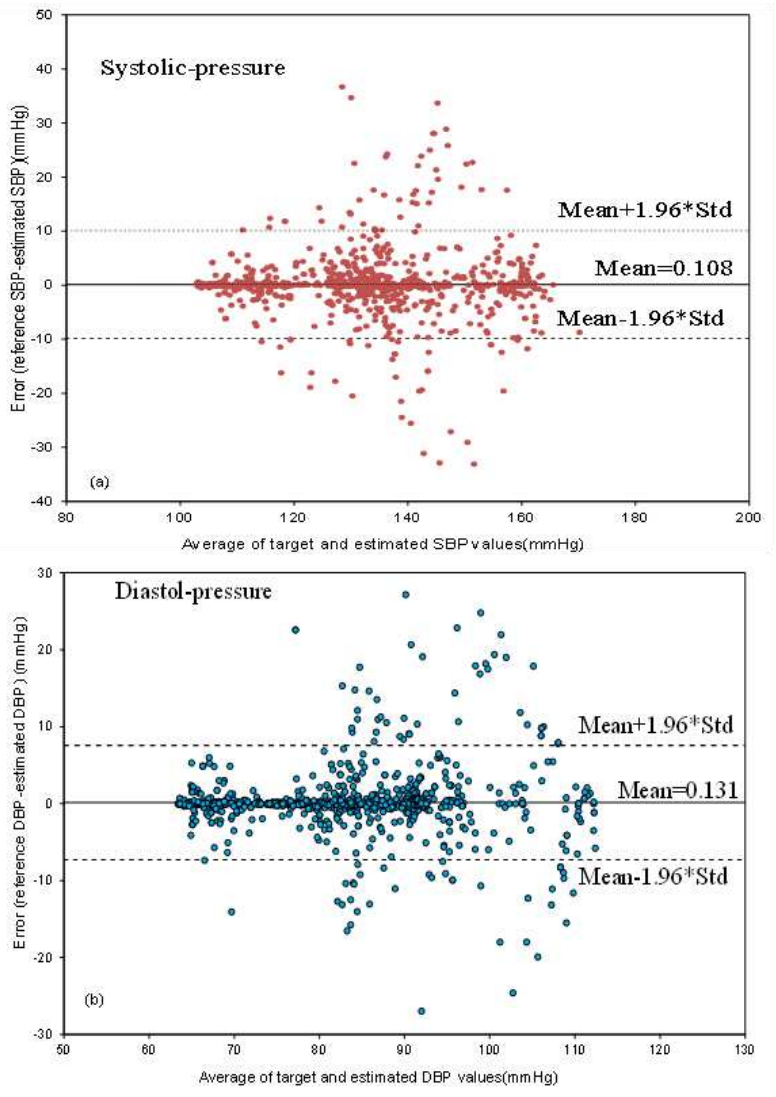


**Fig 8**. Bland-Altman scatter plots for BP value from decision tree. (a) For SBP, (b) for DBP

## 3.2. Comparison with other works

As reported in Table 3, a comparative analysis was performed between the proposed approach and the most-cited works in the literature. Table 3 facilitates the performance evaluation of the suggested method in this study. As appeared in Table 3, the methods which utilize the PPG signal perform the best in terms of BP estimation compared to the methods which use only ECG signal. This reflects the fact that the PPG signal and its various features have a positive effect on improving blood pressure estimation accuracy.

**Table 3**
Comparison of the performance of the proposed method with other works

| work | Estimation Methodology | | Systolic blood pressure | | | Diastolic blood pressure | | |
|---|---|---|---|---|---|---|---|---|
| | Signal | Features | MAE (mmHg) | STD (mmHg) | r | MAE (mmHg) | STD (mmHg) | r |
| [3] | ECG&PPG | PTT&PIR | 7.83 | 9.1 | 0.96 | 4.86 | 5.21 | 0.93 |
| [17] | ECG | Whole-Based Frequency Index | 12.75 | 12.15 | - | 6.04 | 6.42 | - |
| [41] | ECG | Parameter-Based Index | 7.72 | 10.22 | - | 9.45 | 10.03 | - |
| [5] | PCG&PPG | PAT | 6.22 | 9.44 | 0.89 | 3.97 | 5.15 | 0.84 |
| [6] | ECG&PPG | PTT&PIR | 4.09 | 5.21 | 0.91 | 3.18 | 4.06 | 0.88 |
| [12] | ECG&PPG | Parameter-Based Index, PTT | 11.17 | 10.09 | 0.59 | 5.35 | 6.14 | 0.48 |
| [25] | PCG&PPG | PTT | 5.1 | 6.7 | 0.89 | 7.5 | 8.8 | 0.85 |
| This work | PPG | Poincare' Section Index | 2.1 | 5.09 | 0.95 | 1.4 | 3.79 | 0.94 |

Also, to carry out a fair comparison, the capability of the proposed method over the other works that use merely the PPG signal for blood pressure measurement is appraised in Table 4. This comparison was performed based on the results that were reported in the references. It should be noted that most of them used the MIMIC database but with a different subject number. With respect to the results in Table 4, it reveals that this method has a significant performance improvement in BP estimation. The method has minimum error variability (STD) for SBP and DBP values. However, the values of STD for SBP and DBP are more significant than the values in [42]. The cited survey has used feed-forward ANN with two hidden layers and 21 features of time and amplitude characteristic of the PPG signal in the input.

Also, to confirm the potential of the proposed algorithm in BP measurement, the most important parameter-based features from prior reported literature [12] were selected to evaluate with the same data as reported in this work (PPG signal of 101 subjects from the MIMIC database). After extracting parameter-based features, the features were applied to two machine learning algorithms, decision tree and SVM regression. The results are summarized in Table 5. The results convey the fact that, there is no significant difference between the two methods. This comparative test proves

that the Poincaré's section-based features have the equivalent capability in BP measurement to the parameter-based methods.

**Table 4**
Comparison with other works that use only PPG signal

| Work | Estimation Methodology | | | Systolic blood pressure (mmHg) | | | Diastolic blood pressure (mmHg) | | |
|---|---|---|---|---|---|---|---|---|---|
| | Signal | Subject | Features | MAE | STD | ME | MAE | STD | ME |
| [7] | PPG&APG* | 3000 | Parameter-Based | 4.47 | 6.85 | 0.16 | 3.21 | 4.72 | 0.03 |
| [21] | PPG | 41 | Parameter-Based | 4.47 | 6.59 | 4.9 | 2.02 | 3.7 | 2.21 |
| [42] | PPG | 15000*[a] | Parameter-Based | - | 3.46 | 3.8 | - | 2.09 | 2.21 |
| [27] | PPG | 69 | FFT Features | - | 7.08 | 0.06 | - | 4.66 | 0.01 |
| [28] | PPG | 441 | Whole-Based Frequency Index | 3.97 | 8.9 | -0.05 | 2.43 | 4.17 | 0.18 |
| [31] | PPG &APG | 910 | Parameter-Based | - | 10.9 | 8.54 | - | 5.8 | 4.34 |
| [32] | PPG & APG&VPG | 12,000 | Time-Domain Features | 2.4 | 1.01 | - | 3.33 | 1.61 | - |
| [9] | PPG &APG | 111 | Morphological Features and PTT | 4.94 | 5.9 | 0.00 | 4.03 | 5.50 | 0.53 |
| **This Work** | PPG | 101 | Poincare' Section Index | 2.1 | 5.09 | 0.10 8 | 1.4 | 3.79 | 0.13 |

*a) 15000 heartbeat, the number of subjects not reported.*b) 910 good PPG pulse cycle, the number of subjects not reported.

**Table 5**
Comparison of the performance using the two feature sets (proposed method and features from Ref [12]) using two learning algorithms.

| Work | Estimation Methodology | | Systolic blood pressure | | | Diastolic blood pressure | | |
|---|---|---|---|---|---|---|---|---|
| Regression method | Signal | Features | MAE (mmHg) | STD (mmHg) | r | MAE (mmHg) | STD (mmHg) | r |
| **SVM**[12] | PPG | Parameter-Based | 9.9 | 12.34 | 0.61 | 5.5 | 7.54 | 0.73 |
| **Tree**[12] | | | 1.8 | 4.53 | 0.95 | 1 | 3.02 | 0.96 |
| **SVM (This work)** | PPG | Poincare' Section index | 7.9 | 10.64 | 0.74 | 5.04 | 7.15 | 0.77 |
| **Tree (This work)** | | | 2.1 | 5.093 | 0.95 | 1.4 | 3.79 | 0.94 |

## 3.3. Evaluation using the AAMI and BHS Standard

The effectiveness of the current method in BP measurement as a reliable tool is evaluated based on the relevant protocols which are published for "Wearable cuff-less blood pressure measuring devices" in[43]. Based on the mentioned IEEE protocols, STD and MAE are two important criteria of the AAMI and BHS standards. To confirm the performance of the proposed method for cuff-less BP in accordance with the AAMI, the results are summed up in Table 6. Based on the AAMI (ANSI/AAMI SP 10 2002) guideline, the acceptable methods must have a mean error of less than 5mmHg and STD value less than 8 mmHg. Furthermore, the number of subjects participating in the test for evaluating the method accuracy must be greater than 85 [43]. As reflected in Table 6, it is evident that this method fully meets the standard requirement for BP measurement. Also, for evaluating the efficiency of this survey from the viewpoint of the British Hypertension Society (BHS) standard [44], Table 7 has been prepared. According to this standard, BP measurement devices are graded based on their cumulative frequency percentage of errors less than three different thresholds, i.e., 5, 10, and 15 mmHg. In accordance with the qualification criteria of BHS standard, the current algorithm achieves grade A for both DBP and SBP.

**Table 6**
Assessment based on the AAMI Standard

| | | ME (mm Hg) | STD (mm Hg) | Subject |
|---|---|---|---|---|
| AAMI | SBP and DBP | **≤5** | **≤8** | **≥85** |
| This Work | SBP | 0.1 | 5.09 | 101 |
| | DBP | 0.13 | 3.79 | 101 |

**Table 7**
Assessment based on BHS grading system

| | Grade | Cumulative Error Percentage | | |
|---|---|---|---|---|
| | | ≤5 (mm Hg) | ≤10 (mm Hg) | ≤15 (mm Hg) |
| BHS[44] | A | 60(%) | 85(%) | 95(%) |
| | B | 50(%) | 75(%) | 90(%) |
| | C | 40(%) | 65(%) | 85(%) |
| | D | Worse than C | | |
| This Work | SBP | 93.7(%) | 96.78(%) | 97.9(%) |
| | DBP | 95.31(%) | 97.76(%) | 98.81(%) |

## 4. Discussion

Poincaré's section analysis is a well-known nonlinear analysis method and has been used for physiological signal analysis for a long time, especially for heart rate variability. For the first time,

this study used the Poincaré's section analysis of the PPG signal for cuff-less BP estimation. It is also worth noting that the aim of utilizing Poincaré's sections analysis in this paper is to provide a convenient method for feature extraction independent of signal shape, aiming at using only PPG signal for cuff-less BP measurement. One of the main limitations of the prior studies, which used PTT-based methods or parameter-based features of PPG signal for BP measurement, is that the diastolic peak and dicrotic notch on the PPG signal are hard to detect, especially for hypertensive patients [28], and old people which have damped PPG signal [33] . This limitation affects the accuracy of BP estimation and motivated our research to provide a method for estimating BP using PPG signals based on Poincaré's section analysis. The use of Poincaré's section analysis for feature extraction can be a useful and practical solution to mitigate this problem because of any requirement for precise detection of points on the waveform.

To assess the efficiency of this method, compared to other related works, a comparison was performed in Section 3.2. It is noticeable from Table 3 that, in comparison to the other methods, which use ECG or both ECG and PPG signal for BP measurements, our method can estimate SBP and DBP accurately using only PPG signals with the difference of 0.108± 5.09 and 0.13 ± 3.79 mmHg, respectively. The reasonable results of this survey suggest that Poincaré's section-based features have a large potential to be used in BP monitoring, which would bring great benefits for wearable cuff-less BP measurement. We assessed the performance of this method in BP measurement using the MIMIC database. Since this clinical database is a multi-parameter collection based on recordings of ICU patients, therefore, this study is currently limited to clinical data obtained from highly controlled laboratory environments and clinical trials and these results are preliminary and the accuracy of this method have to be confirmed by additional studies on data from healthy people under dynamic test such as cycling. As another important point, in this database some valuable parameters such as age, height and weight of subjects are not reported. Adding these features can improve the accuracy of our method.

As future work, since the lag size is an impressive factor that influences the quality of the phase map and BP estimation accuracy, we are trying to provide a rationale for choosing an appropriate time lag for this study.

## 5. Conclusion

Since almost all the classical PPG based methods, which use time and amplitude-based features, rely on the precise detection of local points and often face the complexity of precise detection or even missing problem particularly in regards to dicrotic notch and diastolic peak, the main focus of our study was to utilize a new PPG based indices for BP estimation. To achieve this goal, the use of the PPG phase space features was investigated in this work, resulting in an easy way to derive reliable features from Poincaré's section analysis. The reported results demonstrate that using Poincaré's sections-based features enhance the precision of the BP estimation algorithm and result in acceptable performance compliant with the British Hypertension Society (BHS) standard. Besides, the results indicate MAE of 2.1 mmHg and 1.4 mmHg for SBP and DBP, respectively, which satisfy entirely the AAMI criteria for BP estimations.

From the results of the investigation carried out on the PPG signal of 101 subjects from the MIMIC database, it can be concluded that Poincaré's section analysis can be a potential solution to extract many informative features from the PPG signal and it paves the way towards developing a wearable BP monitoring system. The proposed method reduces the hardware complexity for cuff-less BP estimation because it does not require finding the local points on the PPG signal precisely, which is a challenging issue.

**Author Contributions**: Authors are equally involved in performing all sections of the article and all of them read and approved the manuscript.

**Funding:** This research did not receive any specific grant from funding agencies.

### Compliance with Ethical Standards

**Conflict of interest:** There is not any conflict of interest.

## References

1. Meng K, Chen J, Li X, et al (2018) Flexible Weaving Constructed Self-Powered Pressure Sensor Enabling Continuous Diagnosis of Cardiovascular Disease and Measurement of Cuffless Blood Pressure. Adv Funct Mater 1806388:1806388. https://doi.org/10.1002/adfm.201806388
2. Rastegar S, GholamHosseini H, Lowe A (2020) Non-invasive continuous blood pressure monitoring systems: current and proposed technology issues and challenges. Phys Eng Sci Med 43:11–28. https://doi.org/10.1007/s13246-019-00813-x
3. Sharifi I, Goudarzi S, Khodabakhshi MB (2019) A novel dynamical approach in continuous cuffless blood pressure estimation based on ECG and PPG signals. Artif Intell Med 97:143–151. https://doi.org/10.1016/j.artmed.2018.12.005
4. Peter L, Noury N, Cerny M (2014) A review of methods for non-invasive and continuous blood pressure monitoring: Pulse transit time method is promising? IRBM 35:271–282. https://doi.org/10.1016/j.irbm.2014.07.002
5. Esmaili A, Kachuee M, Shabany M (2017) Nonlinear Cuffless Blood Pressure Estimation of Healthy Subjects Using Pulse Transit Time and Arrival Time. IEEE Trans Instrum Meas 66:3299–3308. https://doi.org/10.1109/TIM.2017.2745081
6. Ding XR, Zhang YT, Liu J, et al (2016) Continuous Cuffless Blood Pressure Estimation Using Pulse Transit Time and Photoplethysmogram Intensity Ratio. IEEE Trans Biomed Eng 63:964–972. https://doi.org/10.1109/TBME.2015.2480679
7. Gaurav A, Maheedhar M, Tiwari VN, Narayanan R (2016) Cuff-less PPG based continuous blood pressure monitoring - A smartphone based approach. 2016 38th Annu Int Conf IEEE Eng Med Biol Soc 607–610. https://doi.org/10.1109/EMBC.2016.7590775
8. Buxi D, Redouté JM, Yuce MR (2015) A survey on signals and systems in ambulatory blood pressure monitoring using pulse transit time. Physiol Meas 36:R1–R26. https://doi.org/10.1088/0967-3334/36/3/R1

9. Attarpour A, Mahnam A, Aminitabar A, Samani H (2019) Cuff-less continuous measurement of blood pressure using wrist and fingertip photo-plethysmograms: Evaluation and feature analysis. Biomed Signal Process Control 49:212–220. https://doi.org/10.1016/j.bspc.2018.12.006

10. Wang Y, Liu Z, Ma S (2018) Cuff-less blood pressure measurement from dual-channel photoplethysmographic signals via peripheral pulse transit time with singular spectrum analysis. Physiol Meas 39:. https://doi.org/10.1088/1361-6579/aa996d

11. Huynh TH, Jafari R, Chung WY (2018) Noninvasive Cuffless Blood Pressure Estimation Using Pulse Transit Time and Impedance Plethysmography. IEEE Trans Biomed Eng PP:1. https://doi.org/10.1109/TBME.2018.2865751

12. Kachuee M, Member S, Kiani MM, et al (2016) Cuff-Less Blood Pressure Estimation Algorithms for Continuous Health-Care Monitoring. IEEE Trans Biomed Eng 9294:1–11. https://doi.org/10.1109/TBME.2016.2580904

13. Mukkamala R, Hahn J-O, Inan OT, et al (2015) Toward Ubiquitous Blood Pressure Monitoring via Pulse Transit Time: Theory and Practice. IEEE Trans Biomed Eng 62:1879–1901. https://doi.org/10.1109/TBME.2015.2441951

14. Sharma M, Barbosa K, Ho V, et al (2017) Cuff-Less and Continuous Blood Pressure Monitoring : A Methodological Review. Technologies 5:21. https://doi.org/10.3390/technologies5020021

15. Feng J, Huang Z, Zhou C, Ye X (2018) Study of continuous blood pressure estimation based on pulse transit time, heart rate and photoplethysmography-derived hemodynamic covariates. Australas Phys Eng Sci Med 41:403–413. https://doi.org/10.1007/s13246-018-0637-8

16. Thambiraj G, Gandhi U, Devanand V, Mangalanathan U (2019) Noninvasive cuffless blood pressure estimation using pulse transit time, Womersley number, and photoplethysmogram intensity ratio. Physiol Meas 40:. https://doi.org/10.1088/1361-6579/ab1f17

17. Mousavi SS, Hemmati M, Charmi M, et al (2018) Cuff-less blood pressure estimation using only the ECG signal in frequency domain. In: 2018 8th International Conference on Computer and Knowledge Engineering, ICCKE 2018. IEEE, pp 147–152

18. Reisner Andrew MD, Shaltis Phillip A. PD, McCombie D, Asada H Harry PD (2008) Utility of the Photoplethysmogram in Circulatory Monitoring. Anesthesiol J Am Soc Anesthesiol 108:950–958. https://doi.org/10.1097/ALN.0b013e31816c89e1

19. Allen J (2007) Photoplethysmography and its application in clinical physiological measurement. Physiol Meas 28:R1--R39. https://doi.org/10.1088/0967-3334/28/3/r01

20. Li Y, Wang Z, Zhang L, et al (2014) Characters available in photoplethysmogram for blood pressure estimation: beyond the pulse transit time. Australas Phys Eng Sci Med 37:367–376. https://doi.org/10.1007/s13246-014-0269-6

21. Slapničar G, Luštrek M, Marinko M (2018) Continuous blood pressure estimation from PPG signal. Inform 42:33–42

22. Wang G, Atef M, Lian Y (2018) Towards a Continuous Non-Invasive Cuffless Blood Pressure Monitoring System Using PPG: Systems and Circuits Review. IEEE Circuits Syst

Mag 18:6–26. https://doi.org/10.1109/MCAS.2018.2849261

23. El-Hajj C, Kyriacou PA (2020) A review of machine learning techniques in photoplethysmography for the non-invasive cuff-less measurement of blood pressure. Biomed. Signal Process. Control 58:101870

24. Martínez G, Howard N, Abbott D, et al (2018) Can Photoplethysmography Replace Arterial Blood Pressure in the Assessment of Blood Pressure? J Clin Med 7:316. https://doi.org/10.3390/jcm7100316

25. Nemcova A, Jordanova I, Varecka M, et al (2020) Monitoring of heart rate , blood oxygen saturation , and blood pressure using a smartphone. Biomed Signal Process Control 59:101928. https://doi.org/10.1016/j.bspc.2020.101928

26. Ding X-R, Zhao N, Yang G-Z, et al (2016) Continuous Blood Pressure Measurement From Invasive to Unobtrusive: Celebration of 200th Birth Anniversary of Carl Ludwig. IEEE J Biomed Heal Informatics 20:1455–1465. https://doi.org/10.1109/JBHI.2016.2620995

27. Xing X, Sun M (2016) Optical blood pressure estimation with photoplethysmography and FFT-based neural networks. Biomed Opt Express 7:3007–3020. https://doi.org/10.1364/BOE.7.003007

28. Mousavi SS, Firouzmand M, Charmi M, et al (2019) Blood pressure estimation from appropriate and inappropriate PPG signals using A whole-based method. Biomed Signal Process Control 47:196–206. https://doi.org/10.1016/j.bspc.2018.08.022

29. He X, Goubran RA, Liu XP (2014) Secondary peak detection of PPG signal for continuous cuffless arterial blood pressure measurement. IEEE Trans Instrum Meas 63:1431–1439. https://doi.org/10.1109/TIM.2014.2299524

30. Skorobogatova AI, Anisimov AA, Sutyagina AD (2018) The Problem of Pulse Wave Feature Points Detection in Algorithms for Indirect Blood Pressure Estimation. In: 2018 Third International Conference on Human Factors in Complex Technical Systems and Environments (ERGO)s and Environments (ERGO). pp 181–184

31. Liu M, Po L, Fu H (2017) Cuffless Blood Pressure Estimation Based on Photoplethysmography Signal and Its Second Derivative. Int J Comput Theory Eng 9:202–206. https://doi.org/10.7763/ijcte.2017.v9.1138

32. Mohebbian MR, Dinh A, Wahid K, Alam MS (2020) Blind, Cuff-less, Calibration-Free and Continuous Blood Pressure Estimation using Optimized Inductive Group Method of Data Handling. Biomed Signal Process Control 57:101682. https://doi.org/10.1016/j.bspc.2019.101682

33. Xing X, Ma Z, Zhang M, et al (2020) Robust blood pressure estimation from finger photoplethysmography using age-dependent linear models. Physiol Meas 41:. https://doi.org/10.1088/1361-6579/ab755d

34. Goshvarpour A, Goshvarpour A (2018) Poincaré's section analysis for PPG-based automatic emotion recognition. Chaos, Solitons and Fractals 114:400–407. https://doi.org/10.1016/j.chaos.2018.07.035

35. Goldberger AL, Amaral LAN, Glass L, et al (2000) PhysioBank, PhysioToolkit, and PhysioNet. Circulation 101:. https://doi.org/10.1161/01.cir.101.23.e215

36. Chakraborty A, Sadhukhan D, Mitra M (2019) An Automated Algorithm to Extract Time Plane Features From the PPG Signal and its Derivatives for Personal Health Monitoring Application. IETE J Res 0:1–13. https://doi.org/10.1080/03772063.2019.1604178

37. Narayanan SS, Alwan AA (1995) A nonlinear dynamical systems analysis of fricative consonants. J Acoust Soc Am 97:2511–2524. https://doi.org/10.1121/1.411971

38. Sadeghi Bajestani G, Hashemi Golpayegani MR, Sheikhani A, Ashrafzadeh F (2017) Poincaré section analysis of the electroencephalogram in autism spectrum disorder using complement plots. Kybernetes 46:364–382. https://doi.org/10.1108/K-12-2015-0306

39. Fraser AM, Swinney HL (1986) Independent coordinates for strange attractors from mutual information. Phys Rev A 33:1134–1140. https://doi.org/10.1103/PhysRevA.33.1134

40. Lemon SC, Roy J, Clark MA, et al (2003) Classification and Regression Tree Analysis in Public Health: Methodological Review and Comparison with Logistic Regression. Ann Behav Med 26:172–181. https://doi.org/10.1207/S15324796ABM2603_02

41. Simjanoska M, Gjoreski M, Gams M, Bogdanova AM (2018) Non-invasive blood pressure estimation from ECG using machine learning techniques. Sensors (Switzerland) 18:1–20. https://doi.org/10.3390/s18041160

42. Kurylyak Y, Lamonaca F, Grimaldi D (2013) A Neural Network-based method for continuous blood pressure estimation from a PPG signal. In: 2013 IEEE International Instrumentation and Measurement Technology Conference (I2MTC). IEEE, pp 280–283

43. Committee S, Engineering I, Society B (2014) IEEE Standard for Wearable Cuffless Blood Pressure Measuring Devices

44. O'Brien E, Waeber B, Parati G, et al (2001) Blood pressure measuring devices: Recommendations of the European Society of Hypertension. Br Med J 322:531–536. https://doi.org/10.1136/bmj.322.7285.531

# Figures

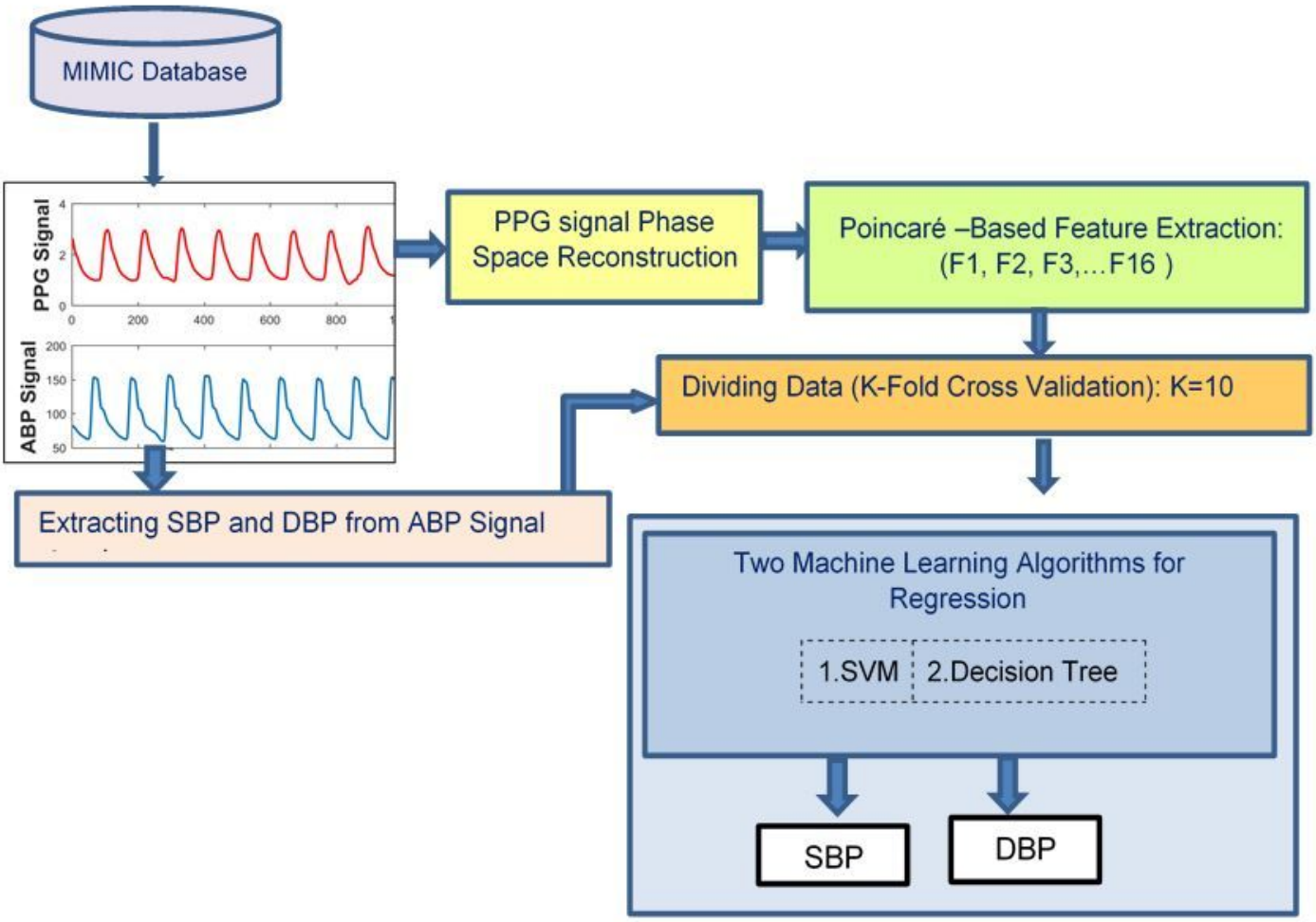


**Figure 1**

Block diagram of the proposed method

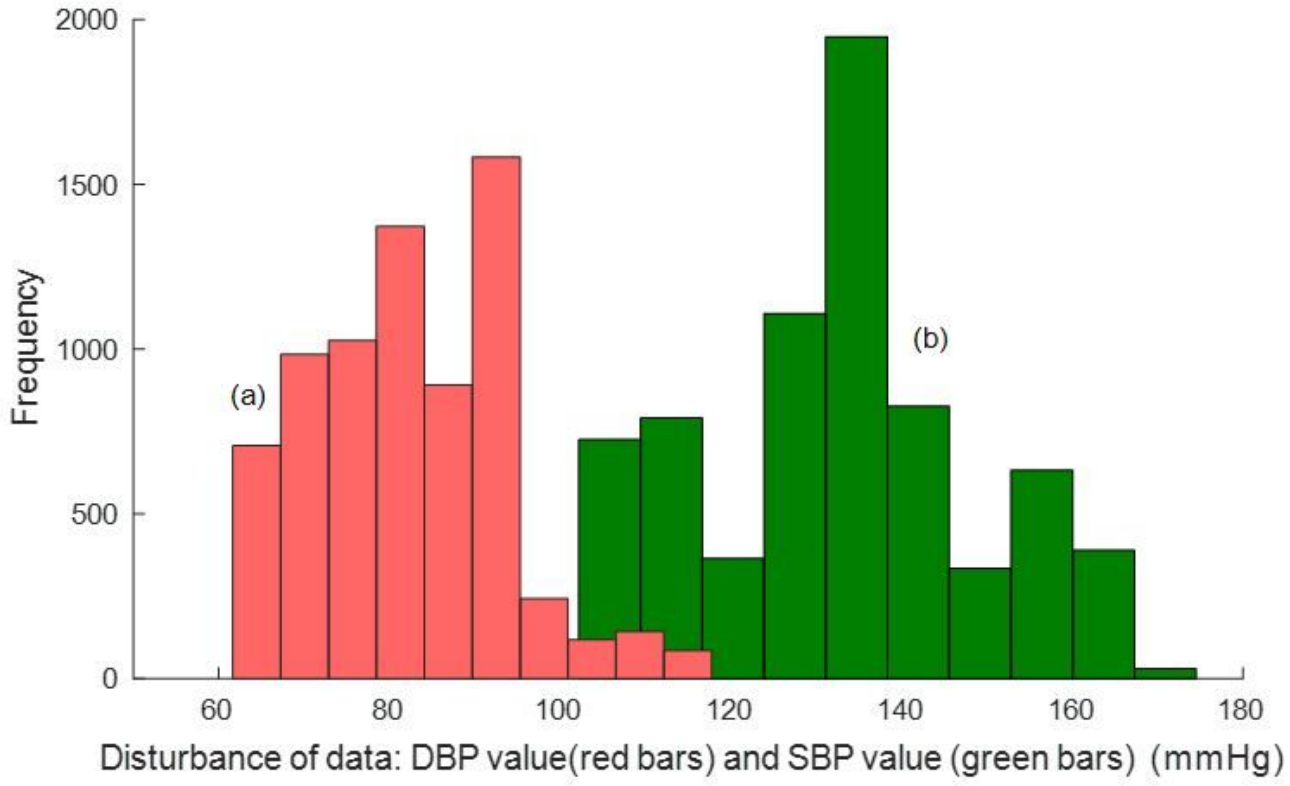


**Figure 2**

Histogram of database (a) DBP (b) SBP

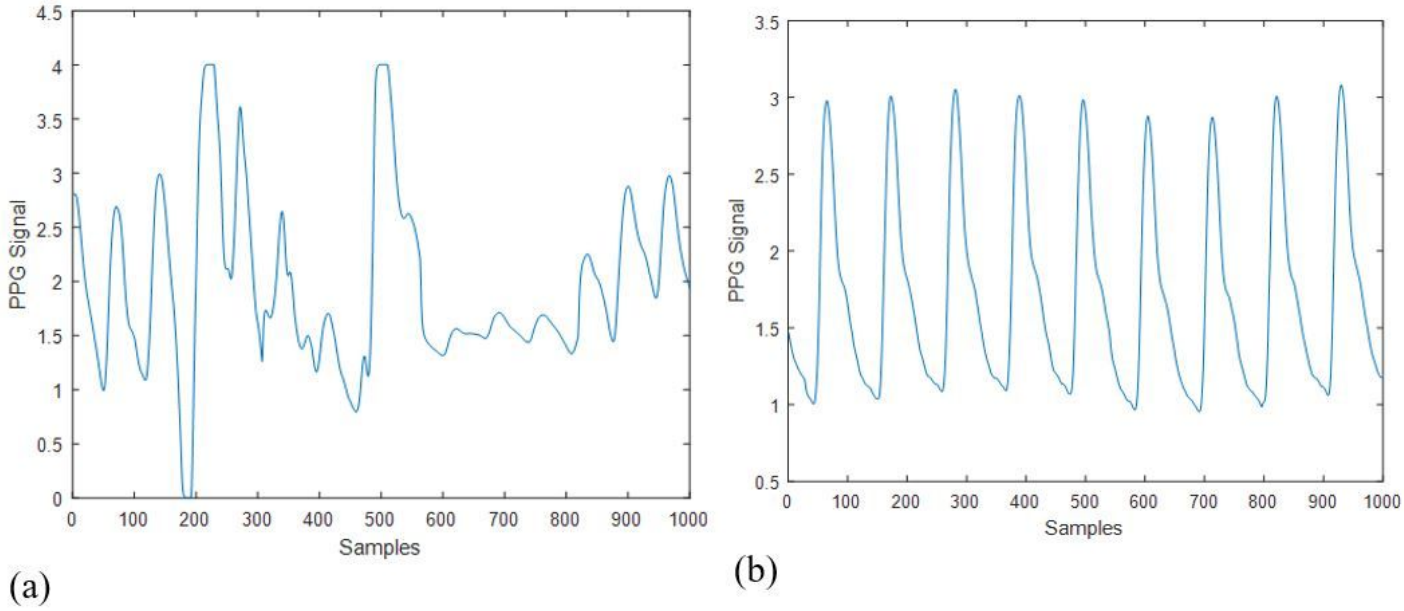


**Figure 3**

An abnormal PPG waveform from MIMIC database (a) normal PPG signal (b)

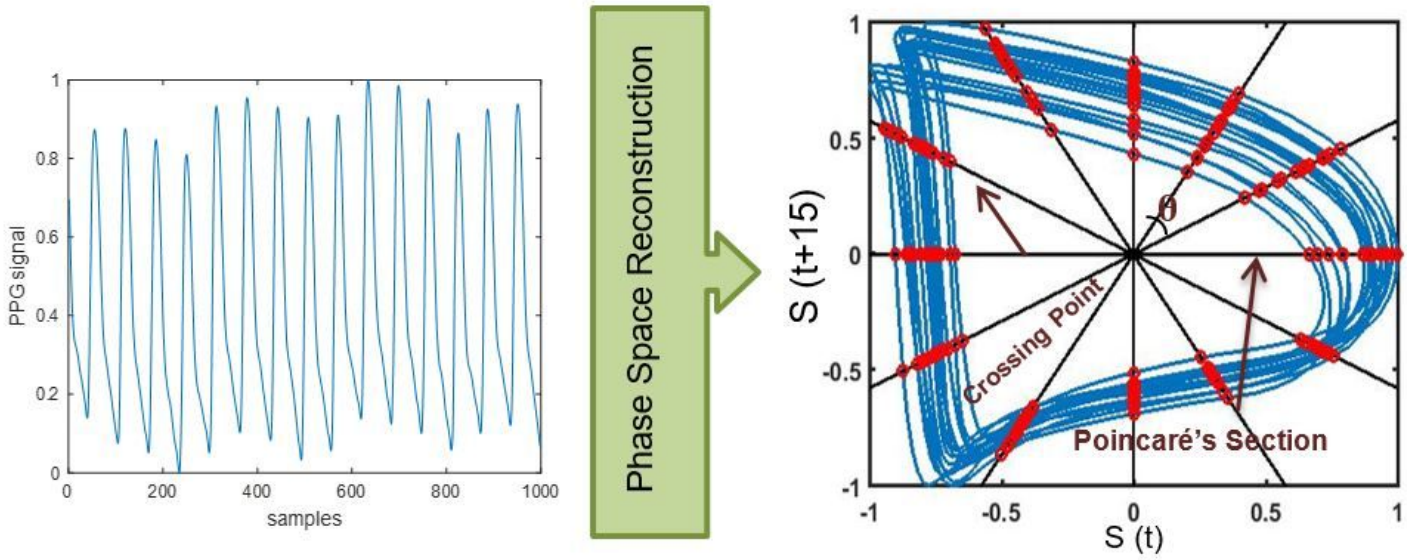


**Figure 4**

The reconstructed phase space and trajectory of one cycle of PPG signal .The black lines refer to Poincaré's sections and the red circles show the crossing points of Poincaré's sections with data trajectory

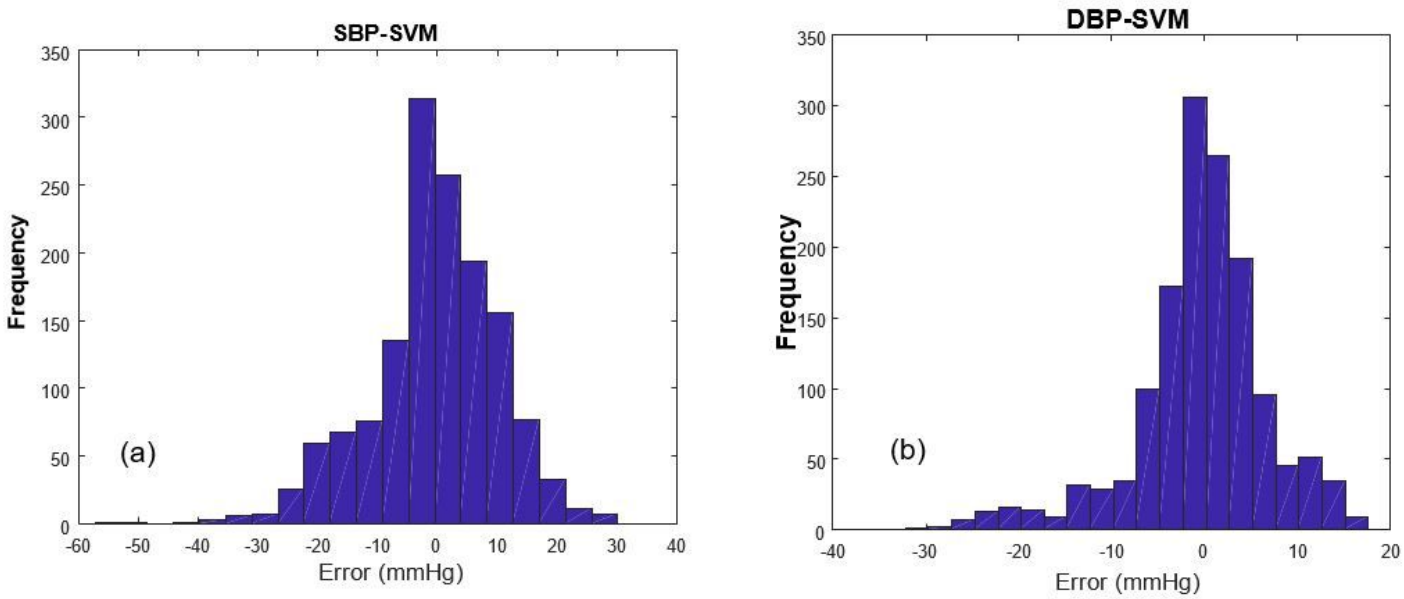


**Figure 5**

BP error histogram from the SVM regression, a) SBP b) DBP

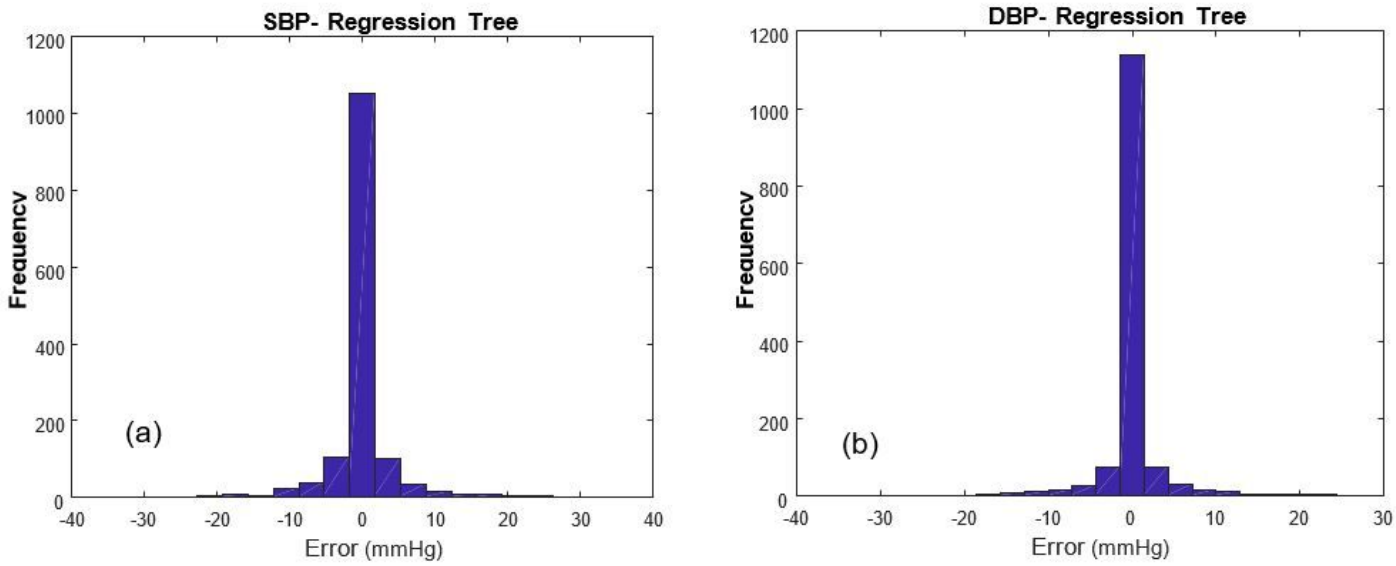


## Figure 6

BP error histogram from the decision tree a) SBP b) DBP

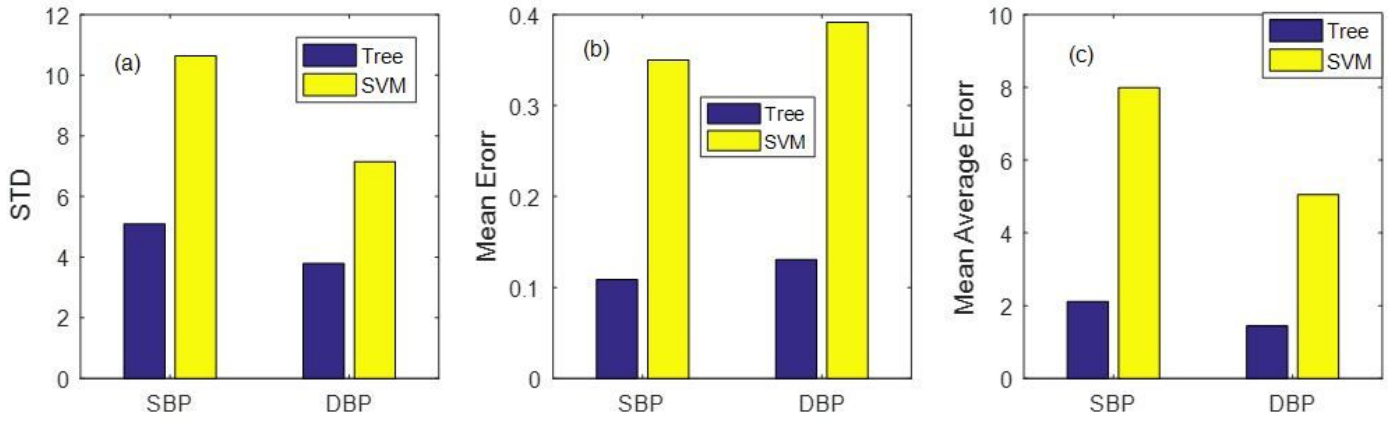


## Figure 7

Comparison of three performance metrics for SVM and Decision Tree a) STD b) ME c) MAE

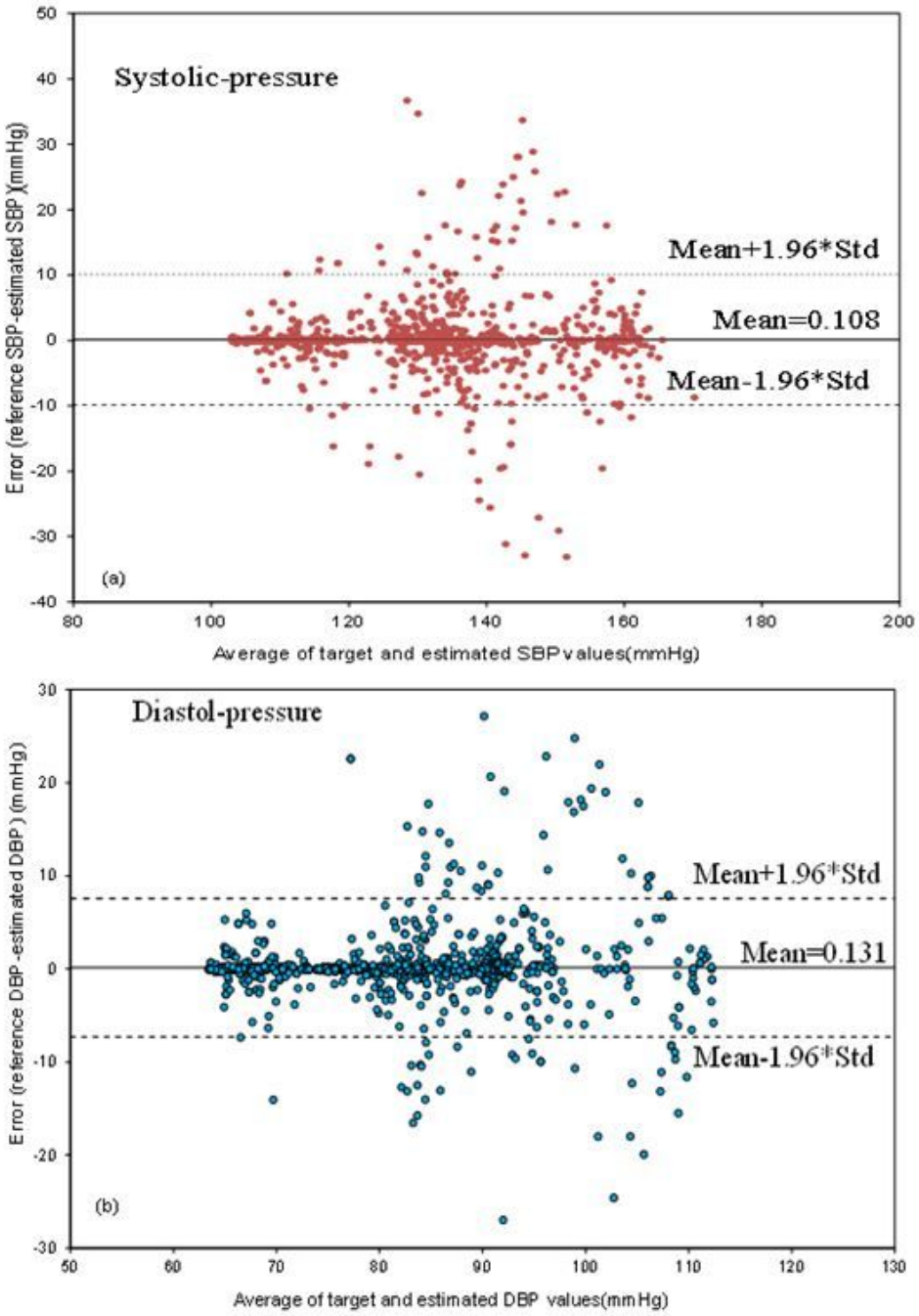


## Figure 8

Bland-Altman scatter plots for BP value from decision tree. (a) For SBP, (b) for DBP